Article

Catalytic Synthesis of 1*H*-2-Benzoxocins: Cobalt(III)-Carbene Radical Approach to 8-Membered Heterocyclic Enol Ethers

Minghui Zhou, Lukas A. Wolzak, Zirui Li, Felix J. de Zwart, Simon Mathew, and Bas de Bruin*
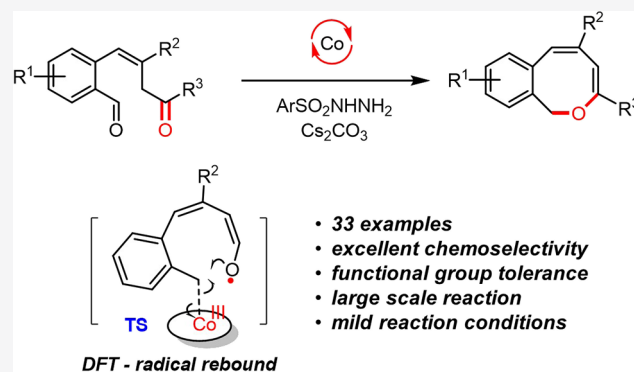
Read Online

ACCESS | Metrics & More | Article Recommendations | Supporting Information

ABSTRACT: The metallo-radical activation of *ortho*-allylcarbonyl-aryl *N*-arylsulfonylhydrazones with the paramagnetic cobalt(II) porphyrin catalyst [Co^{II}(TPP)] (TPP = tetraphenylporphyrin) provides an efficient and powerful method for the synthesis of novel 8-membered heterocyclic enol ethers. The synthetic protocol is versatile and practical and enables the synthesis of a wide range of unique 1*H*-2-benzoxocins in high yields. The catalytic cyclization reactions proceed with excellent chemoselectivities, have a high functional group tolerance, and provide several opportunities for the synthesis of new bioactive compounds. The reactions are shown to proceed via cobalt(III)-carbene radical intermediates, which are involved in intramolecular hydrogen transfer (HAT) from the allylic position to the carbene radical, followed by a near-barrierless radical rebound step in the coordination sphere of cobalt. The proposed mechanism is supported by experimental observations, density functional theory (DFT) calculations, and spin trapping experiments.

- **33 examples**
- **excellent chemoselectivity**
- **functional group tolerance**
- **large scale reaction**
- **mild reaction conditions**

DFT - radical rebound

INTRODUCTION

Medium-sized *O*-heterocycles are important substructures found in several natural compounds with interesting bioactivity toward the cardiovascular and neurological systems of humans (Figure 1).[1,2] Screening a library of related compounds is
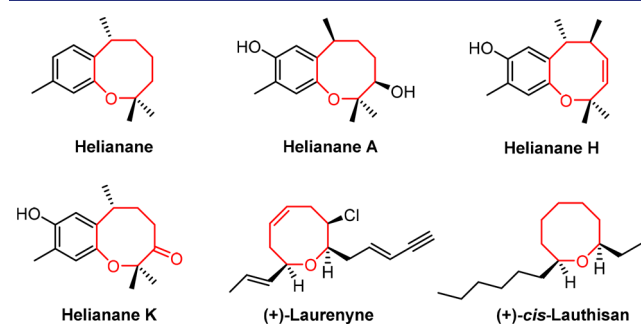

Figure 1. Bioactive 8-membered ether rings.

therefore expected to uncover a range of future pharmaceutical applications. However, such compounds are difficult to synthesize, and as a direct consequence they are largely underrepresented in libraries currently used to screen for bioactivity. Having access to a broad pallet of synthetic possibilities toward these compounds would therefore be helpful in addressing challenges faced in drug discovery, and in particular, novel methods to prepare 8-membered *O*-heterocycles are in high demand. Developing new synthetic
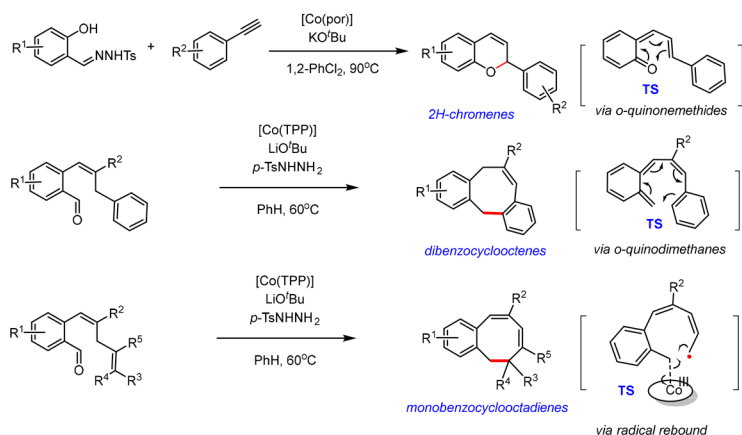
approaches is therefore important. This is not an easy task though, because in contrast to the fruitful synthetic approaches to 5- or 6-membered heterocyclic ring structures, developing synthetic protocols for constructing medium-sized (hetero)-cycles is challenged by entropic factors and inherent trans-annular interactions increasing the transition state barriers. Accordingly, in the synthesis of medium-sized *O*-heterocyclic ring compounds, the applied flexible, linear precursors are generally more amenable to reacting in an intermolecular way, leading to low yields and formation of substantial amounts of unwanted dimerized or polymerized side products. Available protocols for constructing medium-sized ring ethers include ring-closing metathesis,[3] lactone methylenation,[4] reductive cyclization of hydroxyl ketones,[5] Barbier coupling,[6] thermal rearrangement of oxabicyclo[4.2.0] compounds[7] or acylox-ybenzocyclbutenes,[8] Giese radical addition reactions,[9] and ring expansion by Claisen rearrangements.[10] Most of these methodologies require prefunctionalized precursors (such as terminal alkenes in ring-closing metathesis) or multistep synthesis, or they are restricted to specific substrate classes. Additional limitations further confine the applicability of these

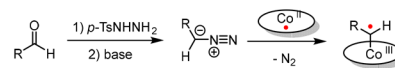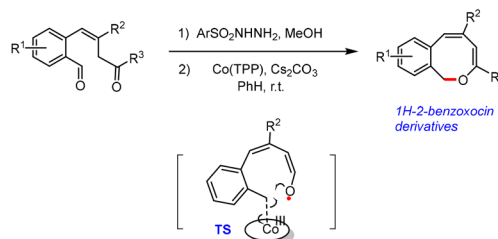**Figure 2.** Design of 8-membered ring ether synthesis by metallo-radical catalysis. A. Previous work in our group utilizing metallo-radical catalysis for the synthesis of 2H-chromenes, dibenzocyclooctenes, and monobenzocyclooctadienes. B. *In situ* generation of cobalt(III)-carbene radical intermediates from aldehydes. C. Present work utilizing cobalt(II) porphyrin ([Co^{II}(TPP), TPP = tetraphenylporphyrin]) catalysis to construct 1H-2-benzoxocins via cobalt(III) carbene radicals.

Table 1. Optimization of the Reaction Conditions
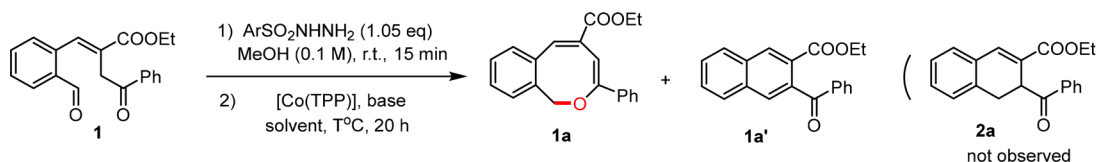
entry[a]	T [°C]	base	solvent	−Ar	yield of 1a[b] (%)	1a/1a'
1[c]	60	LiO^{t}Bu	benzene	−4-MeC$_6$H$_4$	trace	-
2	60	LiO^{t}Bu	benzene	−4-MeC$_6$H$_4$	42	1/1
3	r.t.	LiO^{t}Bu	benzene	−4-MeC$_6$H$_4$	55	1.3/1
4	r.t.	Cs$_2$CO$_3$	benzene	−4-MeC$_6$H$_4$	74	5/1
5	r.t.	KO^{t}Bu	benzene	−4-MeC$_6$H$_4$	57	4/1
6	r.t.	NaOMe	benzene	−4-MeC$_6$H$_4$	9	0.8/1
7	r.t.	Cs$_2$CO$_3$	chlorobenzene	−4-MeC$_6$H$_4$	67	4/1
8	r.t.	Cs$_2$CO$_3$	1,2-dichlorobenzene	−4-MeC$_6$H$_4$	71	5/1
9	r.t.	Cs$_2$CO$_3$	benzene	−2,4,6-^{i}PrC$_6$H$_4$	**83**	6.5/1
10	r.t.	Cs$_2$CO$_3$	benzene	−4-OMeC$_6$H$_4$	**84**	6.2/1
11	r.t.	Cs$_2$CO$_3$	benzene	−3-NO$_2$C$_6$H$_4$	65	5/1
12	r.t.	Cs$_2$CO$_3$	benzene	−2-ClC$_6$H$_4$	75	5/1
13[d]	r.t.	Cs$_2$CO$_3$	benzene	−4-OMeC$_6$H$_4$	36	2/1
14[e]	r.t.	Cs$_2$CO$_3$	benzene	−4-OMeC$_6$H$_4$	42	2/1.5

[a]Reaction conditions: Substrate **1** (0.1 mmol, 1.0 equiv) and the arylsulfonyl hydrazide (0.105 mmol, 1.05 equiv) were mixed in methanol (1.0 mL), and stirred for 15 min at room temperature. The thus-obtained crude hydrazone (= carbene precursor) (0.1 mmol) was mixed with [Co(TPP)] (0.005 mmol, 0.05 equiv) and base (0.11 mmol, 1.1 equiv) in benzene (1.0 mL), and stirred at room temperature for 20 h. [b]Yields were determined by integration of the ^{1}H NMR signals in the presence of dimethyl sulfone as internal standard. [c]Substrate **1** (0.1 mmol, 1.0 equiv), the arylsulfonyl hydrazide (0.105 mmol, 1.05 equiv), [Co(TPP)] (0.005 mmol, 0.05 equiv) and base (0.11 mmol, 1.1 equiv) were directly mixed in benzene (1.0 mL) in a one-pot reaction, and the mixture was stirred at 60 °C for 20 h. [d][Co(ppIX)] (0.003 mmol, 0.03 equiv) and Aliquat 336 (0.015 mmol, 0.15 equiv) were used instead of Co(TPP). [e][Co(ppIX-OMe)] (0.003 mmol, 0.03 equiv) and 4-DMAP (0.005 mmol, 0.05 equiv) were used instead of [Co(TPP)].

strategies, such as harsh reaction conditions, unavoidable byproduct generation, and the necessity of noble metal catalysts. Therefore, developing new, efficient strategies to synthesize 8-membered O-heterocycles remains an important task.

In recent years, catalytic radical-type transformations have proven to be attractive methods in the construction of cyclic products,[11] and one outstanding example is the application of Co(II)-based metallo-radical catalysis in ring-closing synthesis. In particular, square-planar cobalt-porphyrin complexes with well-defined open-shell doublet ($S = 1/2$) low-spin d^7-

electronic configuration display a remarkable radical-type reactivity.[12] In carbene transfer reactions mediated by these systems, the cobalt(II) complex catalyst first reacts with a carbene precursor[13] (such as a diazo compound or a N-phenyl-sulfonohydrazone, Figure 2B), and then transforms to a cobalt(III)-carbene radical intermediate by an intramolecular metal-to-substrate single-electron transfer from cobalt(II) to the carbene carbon atom. The carbene carbon atom in cobalt(III)-carbene radical intermediate is a carbon-centered radical involved in subsequent radical-type reaction pathways. This metallo-radical strategy has been successfully employed in

the synthesis of ring structures, such as cyclopropanes,[14] furans,[15] indenes,[16] indolines,[17] ketenes,[18] dihydronaphthalenes,[19] piperidines,[20] and pyrrolidines.[21] Furthermore, an efficient synthetic protocol for the synthesis of 2*H*-chromenes has been developed (Figure 2A),[22] and we also successfully applied the intrinsic radical-type reactivity of cobalt(III)-carbene radicals to construct two types of new 8-membered carbocyclic compounds: dibenzocyclooctenes[23] and mono-benzocyclooctadienes[24] (Figure 2A). Building on these prior results, and in view of our continued interest in cobalt(II)-based metallo-radical catalysis, we envisioned that related open-shell catalysis could also uncover new possibilities for the synthesis of 8-membered *O*-heterocyclic compounds (Figure 2C).

Herein, we describe a highly effective metallo-radical approach to construct 8-membered oxygen heterocycles via cobalt(III)-carbene radical mediated cyclization. This protocol affords a class of unprecedented 1*H*-2-benzoxocins. DFT calculations suggest that the cyclization to 1*H*-2-benzoxocins proceeds via a unique reaction sequence involving a 1,6-HAT followed by a radical-rebound process leading to C−O bond formation directly in the coordination sphere of cobalt. This new methodology produces the novel heterocyclic products efficiently, under mild reaction conditions, and exhibits a broad substrate scope and high functional group tolerance. In addition, this reaction is easy to scale up and the *O*-heterocyclic products can be functionalized with various bioactive substituents.

■ RESULTS AND DISCUSSION

Inspired by previous work on metallo-radical catalysis in cyclization reactions, we continued our research by seeking a new synthetic approach to 8-membered *O*-heterocycles. As such, we designed a substrate with an allylcarbonyl moiety, and began our study by using **1** as the model substrate to probe the feasibility of ring-closure to the desired 8-membered ring compound **1a** (Table 1). At first, we tested the reaction using LiO*t*Bu as the base and *p*-TsNHNH₂ to prepare the hydrazone from the aldehyde *in situ*. The reaction was performed at 60 °C in one pot (Table 1, entry 1). However, under these conditions we obtained only a trace amount of the desired cyclic product **1a**, while the aromatic 6-membered ring product **1a′** was obtained as the main product instead. This result was unexpected, and formation of naphthalene **1a′** seems to be the result of an uncatalyzed intramolecular aldol condensation reaction of aldehyde substrate **1**, producing the aromatic product upon elimination of water (Scheme 1, red pathway).[25]
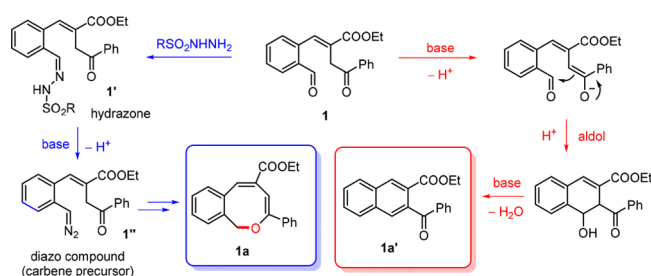
Indeed, a control reaction in the absence of the [Co(TPP)] catalyst also produced **1a′** in 95% yield (see Figure 5). Under the catalytic conditions, this side reaction seems to take place before **1** has the chance to react properly with the arylsulfonyl hydrazide to produce the diazo compound (Scheme 1, blue pathway), thus preventing the desired metallo-radical cyclization to **1a**.

To constrain this side reaction, we therefore adjusted the experimental procedure by preparing the hydrazone **1′** first, in the absence of added base, and then using the crude hydrazone as a carbene precursor for the catalytic reaction (Scheme 1). To our delight, under these conditions the desired 8-membered enol ether ring-product could be obtained in a much higher yield (Table 1, entry 2).

Lowering the reaction temperature increased the selectivity for the desired product further (Table 1, entry 3). After screening various bases and solvents, Cs₂CO₃ was found to be the most suitable base to trigger the reaction (Table 1, entries 4−6). Changing to solvents with a somewhat higher polarity proved to have only a small influence on the yield of **1a** (Table 1, entries 4, 7, and 8). Further evaluation using differently substituted arylsulfonyl hydrazides revealed that *p*-methoxy-benzenesulfonyl hydrazide and 2,4,6-triisopropylbenzenesulfonyl hydrazide work best (Table 1, entries 9−12). To explore the importance of the *meso*-substituents on the porphyrin ligand we also tested the bioderived [Co^II(ppIX)] and [Co^II(ppIX-OMe)] catalysts (ppIX = protoporphyrin IX; ppIX-OMe = methyl ester of ppIX) lacking *meso*-substituents (Table 1, entries 13 and 14). These catalysts also produce the desired 8-membered product **1a**, albeit in a moderate yield. We ascribe the lower yields to self-aggregation of these catalysts in solution. Nonetheless, *meso*-substituents on the porphyrin ring are clearly not essential for the reaction. Interestingly, the 6-membered dihydronaphthalene ring product **2a** was not observed in the whole series of optimization reactions, while its formation by carbene insertion into the allylic C−H bond was expected to be feasible and competitive, based on both thermodynamic considerations and an expected easier cyclization to 6-membered rings than to 8-membered rings (for entropic reasons and due to transannular interactions). Formation of **1a** in high yields is in fact not trivial at all, as besides formation of **1a′** instead of the expected 6-membered ring product **2a**, the instability of the substrate under both acidic and basic conditions (caused by the reactive α-H position of the allylcarbonyl moiety) could have led to a variety of other unwanted side reactions. Ring-closure reactions involving (formal) carbene addition to a ketone group are rare in general,[26] and ring-closure of a carbene precursor onto a ketone group to produce an 8-membered *O*-heterocycle is unprecedented.

With the optimal reaction conditions being established, we started to evaluate the generality of the new cyclization protocol. First, different substituents on the R¹ = aryl moiety were evaluated. Pleasingly, these substrates were compatible with this reaction as well and afforded a broad range of new 8-membered *O*-heterocyclic products (Figure 3A). It seems that substrates with electron-donating substituents on the R¹ = aryl ring result in a somewhat higher yield of the desired 8-membered products (Figure 3A: **2a**) than substrates substituted with electron-withdrawing groups (Figure 3A: **3a−9a**).[27]

No obvious influence of the position of the substituents on the yields was observed. Substrates with bulkier groups at the

Scheme 1. Desired Formation of 8-Membered *O*-Heterocycle 1a via Hydrazone 1′ and Diazo Compound 1″ (blue) versus Undesired Formation of Naphthalene 1a′ via an Aldol Condensation Pathway (Red)
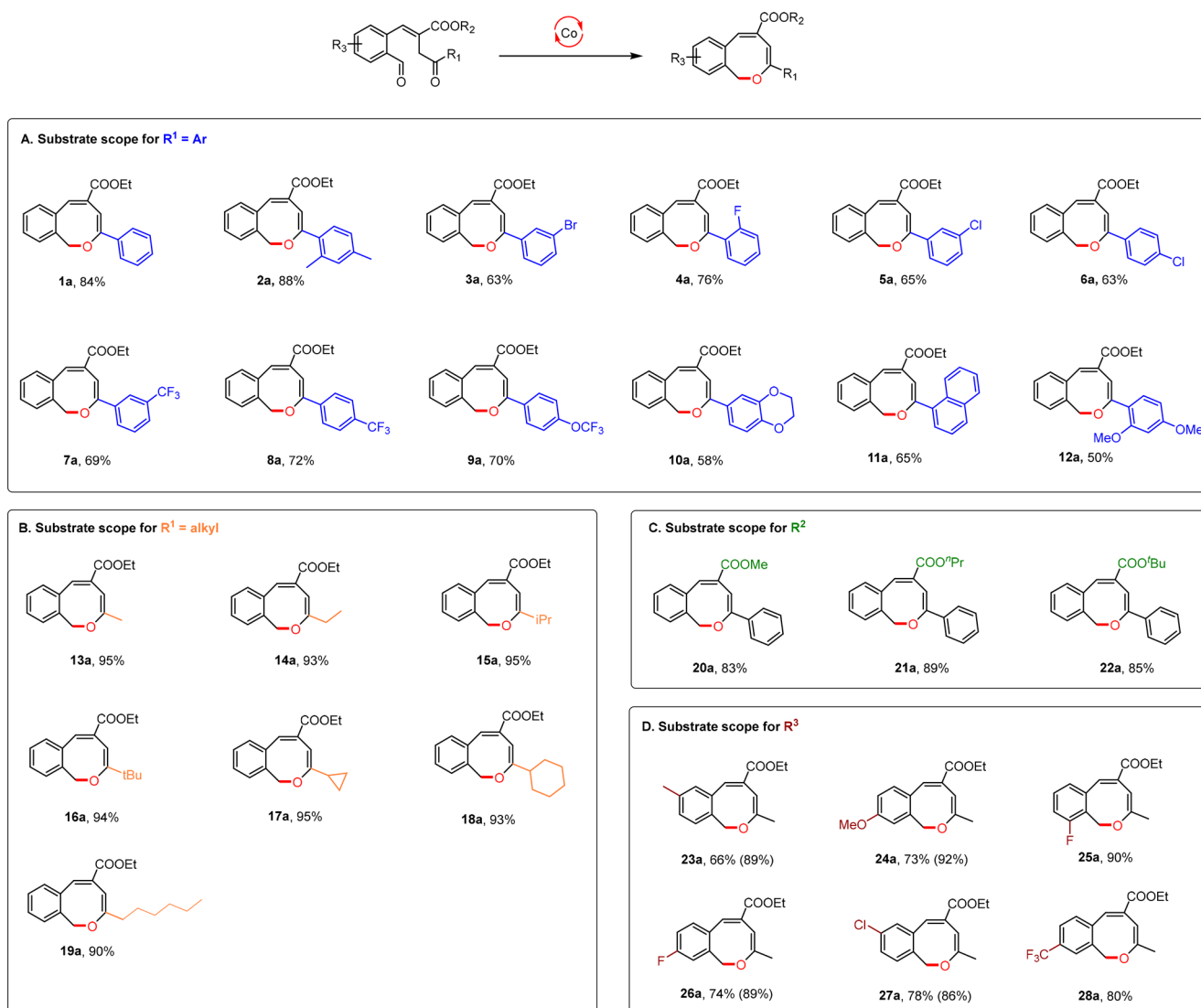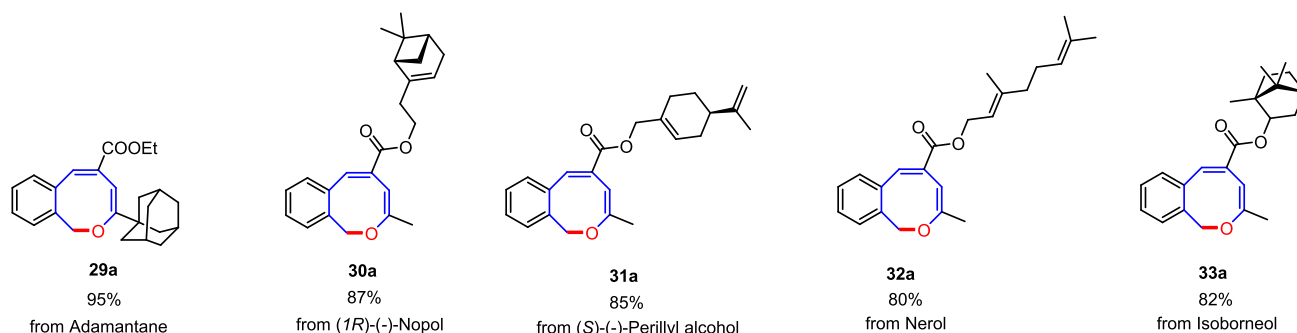
Figure 3. Substrate scope for formation of 1H-2-benzoxocins. Standard reaction conditions: the substrates (0.1 mmol, 1.0 equiv), p-methoxybenzenesulfonyl hydrazide (0.105 mmol, 1.05 equiv) were mixed in methanol (1.0 mL) and stirred for 15 min at room temperature; The thus obtained crude hydrazones (= carbene precursors) (0.1 mmol) were mixed with [Co(TPP)] (0.005 mmol, 0.05 equiv) and Cs_2CO_3 (0.11 mmol, 1.1 equiv) in benzene (1.0 mL), and stirred at room temperature for 20 h. Isolated yields are shown. For **23a**, **24a**, **26a**, and **27a**, the isolated yields corrected for the E/Z ratio of the substrates are shown between parentheses.
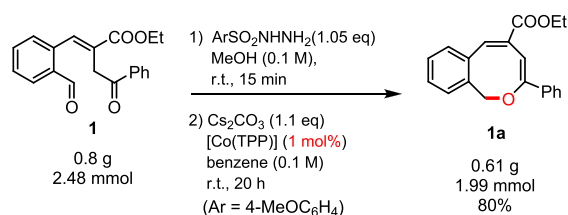
aromatic R^1 position seem to reduce the chemoselectivity slightly (Figure 3A: **1a**, **10a**, and **11a**, yield drops from 84% to around 60%), and in those cases a bit more of the aromatic aldol side products were formed, thus lowering the yield of the desired 8-membered ring products. We also noticed that some of the 8-membered enol ether ring products are rather unstable. This is the case for **12a**, which decomposes rapidly, and as a result this compound was always obtained as a mixture containing a small amount of unidentifiable decomposition products, which is possibly due to the increased electron density of the enol moiety. However, in general the protocol works well for various substrates with different R^1 = aryl moieties and affords the 8-membered ring products in yields between 50% and 88%.

We continued our investigation of the substrate scope by changing the aryl groups adjacent to the carbonyl moiety to aliphatic groups (Figure 3B). As the carbonyl moiety is directly involved in the cyclization process, changing substituents on the carbonyl from aryl to alkyl could affect the geometry and

electron distribution of the intermediates and transition states, and hence could in principle have a substantial influence on the outcome of the reaction. A change in mechanism could even lead to a switch of the preferred reaction pathway, for example, leading to preferred formation of 6-membered ring products such as dihydronaphthalenes. However, formation of 8-membered cyclic products was still the preferred pathway for these substrates, and the selectivity over 6-membered naphthalene ring formation proved to be even better for R^1 = alkyl than for R^1 = aryl substrates. Almost no aldol cyclization products could be detected in these reactions, and the desired 8-membered heterocycles were obtained in near-quantitative yield. Even bulky alkyl substituents do not hinder the reaction (Figure 3B: **15a–19a**). Notably, the substrates containing cyclopropyl and cyclohexyl moieties also smoothly reacted to produce the desired 8-membered enol ethers in high yield, and no cyclopropyl or cyclohexyl ring-opened products were observed (Figure 3B: **17a** and **18a**).

A. Synthesis of 1H-2-benzoxocins containing biologically relevant substituents

29a
95%
from Adamantane

30a
87%
from (1R)-(-)-Nopol

31a
85%
from (S)-(-)-Perillyl alcohol

32a
80%
from Nerol

33a
82%
from Isoborneol

B. Larger scale reaction

1
0.8 g
2.48 mmol

1) ArSO$_2$NHNH$_2$(1.05 eq)
MeOH (0.1 M),
r.t., 15 min

2) Cs$_2$CO$_3$ (1.1 eq)
[Co(TPP)] (1 mol%)
benzene (0.1 M)
r.t., 20 h
(Ar = 4-MeOC$_6$H$_4$)

1a
0.61 g
1.99 mmol
80%

C. Molecular structure of 27a
(obtained by x-ray diffraction)
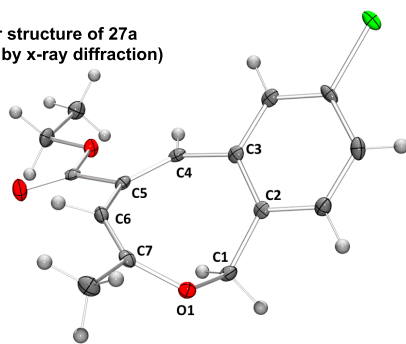
D. Synthetic transformations of 1H-2-benzoxocins

19aa, 85%

13ab, 67%

19ac, 80%

19ad, 82%

19ae, 95%

19af, 75%
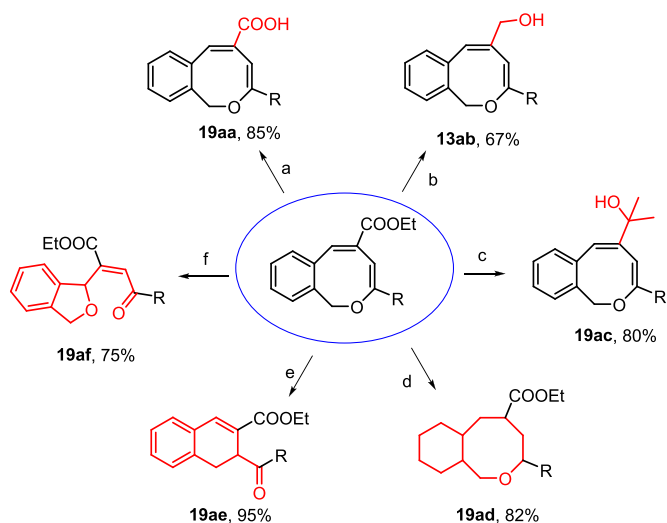
Figure 4. Synthetic practicality and applications of 1H-2-benzoxocins. A. Modification of pharmaceutical derivatives and natural products. B. Larger-scale reaction. C. Molecular structure of **27a** (ORTEP diagram with 50% probability ellipsoids), as determined by single crystal X-ray diffraction. Selected bond distances [Å] for **27a**: C1−C2 1.502(4); C2−C3 1.401(4); C3−C4 1.468(3); C4−C5 1.348(4); C5−C6 1.474(5); C6−C7 1.335(4); C7−O1 1.367(3); C1−O1 1.440(4). D. Synthetic transformation of 1H-2-benzoxocins. Start from **13a** or **19a**. (a) NaOH (2.0 equiv); H$_2$O/MeOH; 40 °C, 8 h. (b) Diisobutylaluminum hydride (3.0 equiv); DCM; −78 °C to room temperature; 2 h. (c) Methylmagnesium bromide (2.0 equiv); THF; 0 °C; 1 h. (d) H$_2$ (1 bar); Rh/Al$_2$O$_3$; MeOH; room temperature; 20 h. (e) Toluene; 120 °C, 3 d. (f) Al$_2$O$_3$ (10.0 equiv); NaOCl (3.0 equiv); MeCN, 0 °C; 2 h.

To further expand the scope, substrates with different ester groups were synthesized and tested. Gratifyingly, changing the ester groups has little effect on the reactivity, and all desired 8-membered cyclic products were obtained in good yields (Figure 3C). We continued to screen the substrate scope of the reaction by checking the feasibility of different R^3 substituents at the phenyl ring of the benzaldehyde moiety. Various R^3 substituents also proved to be well-tolerated, and products **23a−28a** were obtained in yields between 80% and 92% (Figure 3D).

Note that most of the results listed in Figure 3 were obtained using pure E-isomers of the substrates. Only a small amount of Z-isomer was found in substrates **23**, **24**, **26**, and **27**. The isolated yields of **23**, **24**, **26**, and **27** corrected for the E/Z ratio of these substrates are shown between parentheses in Figure 3 because only the E-isomer can convert to the final 8-membered ring.[23,24]

The broad substrate scope demonstrated in Figure 3 reveals an exceptional functional group tolerance and high efficiency toward formation of medium-sized ring structures, which offers several possibilities to prepare 8-membered O-heterocycles containing biologically relevant substituents. Hence, to further explore the practicability of the protocol, we employed the cobalt-catalyzed cyclization reaction to synthesize the 1H-2-benzoxocins functionalized with different bioactive and druglike substituents shown in Figure 4A. The compounds in Figure 4A were obtained in good yields, using the aforementioned standard reaction conditions. Notably, some of the substrates used in these reactions contain functional groups that are known to be sensitive to intra- or intermolecular radical attack, but the desired 8-membered ring products were still obtained in high yields, which demonstrates the excellent chemoselectivity toward formation of 8-membered O-heterocyclic enol ethers.
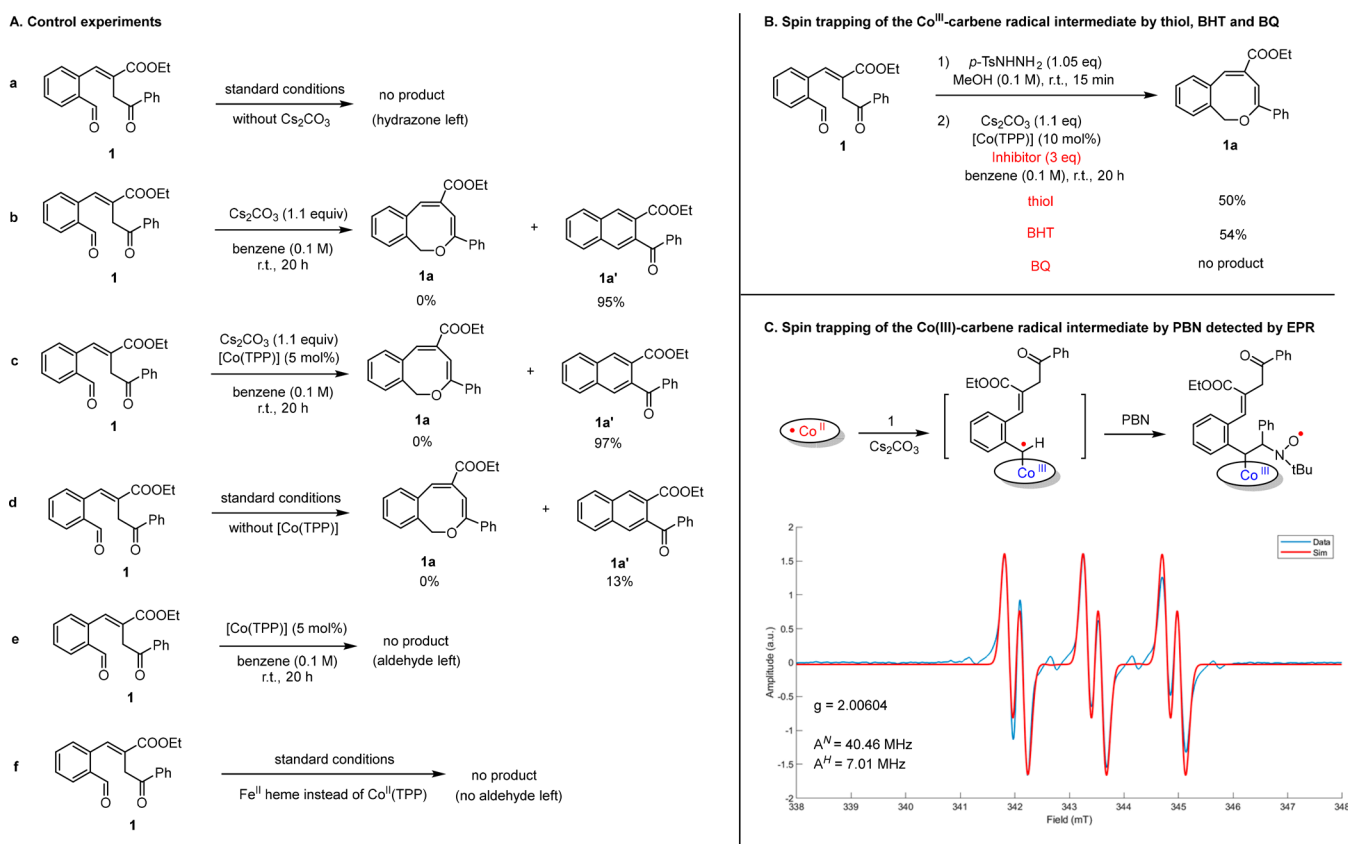
Figure 5. Mechanistic studies. A. Control experiment. B. Spin trapping of the cobalt(III)-carbene radical intermediate by thiol, BHT, and BQ. C. Spin trapping of the cobalt(III)-carbene radical by PBN, detected with EPR spectroscopy.

To demonstrate that larger quantities can be synthesized with the newly developed protocol, we also tested the reaction on a near-gram scale (Figure 4B), showing that the 8-membered O-heterocycle **1a** is still obtained in a high yield even when using a lower catalyst loading of 1 mol % (no other changes in reaction conditions).

The molecular structure of 1H-2-benzoxocin **27a** was confirmed by single crystal X-ray diffraction (Figure 4C). Single crystals of **27a** were harvested upon solvent evaporation of an NMR sample to dryness after chromatography. Compound **27a** crystallized in the monoclinic space group $P2_1/n$. Notably, the C7−O1 bond length (1.367(3) Å) in the newly generated heterocycle is much shorter than that of C1−O1 (1.440(4) Å) in **27a**, showing that C7 is sp^2 hybridized, while C7−O1 may also feature some double-bond character.

Considering that the products generated in this reaction contain unusual 8-membered ring structures with a conjugated acrylate moiety and special enol ring motif, we argued that these compounds are likely to be interesting substrates for further transformations. As such, we explored the reactivity of compounds **19a** and **13a** as model substrates, showing a broad reactivity pattern (Figure 4D). **19a** could be efficiently hydrolyzed under mild conditions to produce the carboxylic acid product **19aa**. Reduction of the ester moiety of **13a** with DIBAL-H produced the allylic alcohol **13ab** in high yield, and reaction of **19a** with the Grignard reagent MeMgBr efficiently produced the corresponding substituted alcohol **19ac**. Note that both the DIBAL-H reduction and Grignard reaction are highly chemoselective and do not affect the alkene and enol motifs. **19a** could also be hydrogenated by a heterogeneous Rh

catalyst, producing the fully hydrogenation product **19ad**. Interestingly, heating the 8-membered enol ring compound **19a** to 120 °C for 3 days converted the 8-membered ring compound to the thermodynamically more stable 6-membered ring product, namely, dihydronaphthalene **19ae**. We ascribe formation of **19ae** to thermal ring opening of **19a** to the corresponding *ortho*-quinodimethane (*o*-QDM) compound, followed by cyclization to **19ae** (Scheme 3 in reserve). Note that substituted dihydronaphthalenes are key motifs in many bioactive compounds, but are in fact also difficult to construct via existing organic synthetic methods.[28] Interestingly, reaction of **19a** with sodium hypochlorite in the presence of neutral alumina also leads to a selective ring-contraction, but in this case to the 5-membered ring product 1,3-dihydroisobenzofuran-3-oxobutanoate **19af**. The exact mechanism of this reaction is presently unclear, but it should be noted that 1,3-dihydroisobenzofuran-3-oxobutanoates are important bioactive substructures found in the vaccinol family of compounds (vaccinol H and vaccinol I),[29] and **19af** is also an analogue of emefuranone and emefuran, which are bioactive secondary metabolites of a diverse genus of filamentous fungi that have potent antimicrobial activity.[30] Until now, no organic synthetic methods to prepare these type of compounds have been reported, and this is in fact the first reported efficient laboratory route to 1,3-dihydroisobenzofuran-3-oxobutanoates. These proof-of-principle transformations demonstrate that the 8-membered enol ether ring structures provide powerful platforms to synthesize a variety of potentially bioactive compounds. While screening for biological activity is beyond the scope of the present paper, it could well be worthwhile to test these compounds, as well as the 1H-2-benzoxocins, for

Scheme 2. Proposed Mechanism for the [Co(porphyrin)]-Catalyzed Formation of 1*H*-2-Benzoxocins, Based on DFT Calculations (BP86, def2-TZVP, m4 grid, disp3)[a]
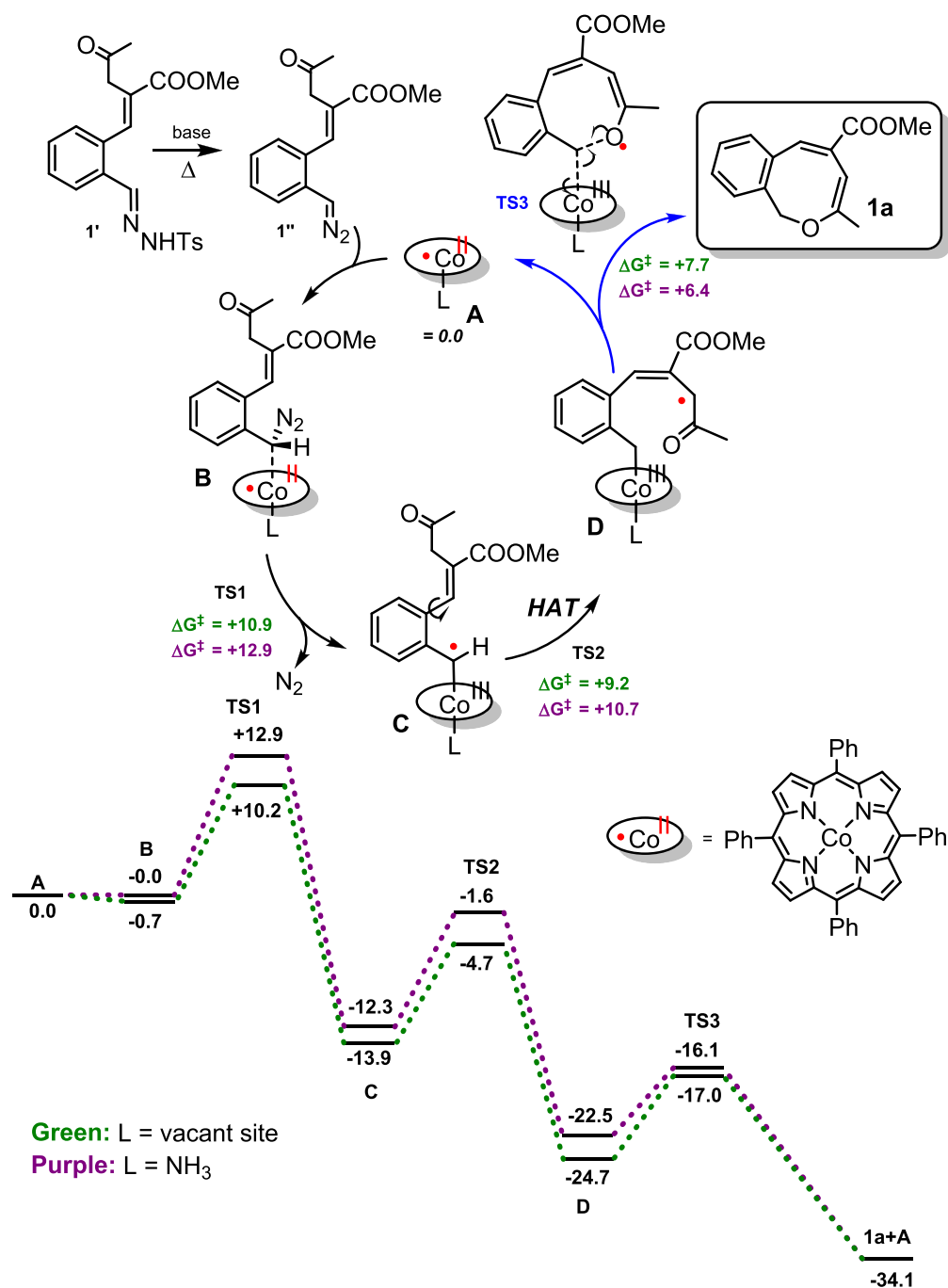
[a]All Gibbs free energies ($\Delta G^{\circ}_{298\,K}$ in kcal mol^{-1}), including those of TS1–TS3, are reported relative to the energy of intermediate A. Full atom models.

potential pharmaceutical applications in follow-up studies. Further synthetic applications are ongoing in our lab.

Mechanistic Investigations. Several control experiments were performed to obtain a better understanding of the reaction mechanism (Figure 5). The base is indispensable to trigger the desired catalytic reaction (Figure 5A, a), but direct contact between the base and the aldehyde in the reaction mixture is also the principal reason for the formation of the aldol side product (Figure 5A, b and c). Formation of the desired 8-membered enol ether ring product was not observed in the absence of hydrazide (Figure 5A, c), and using the

preformed hydrazone as the carbene precursor (instead of mixing aldehyde + hydrazide) strongly inhibits the unwanted aldol side reaction (Figure 5A, b and d). Due to the reversibility of hydrazone−aldehyde equilibrium, a small amount of intramolecular aldol cyclization product still occurs, depending on the structure of the substrates (Figure 5A, b and d).

The cobalt catalyst is not involved in the aldol side reaction (Figure 5A, b, c, and d), and it also does not activate the aldehyde precursor directly (Figure 5A, c). Only after deprotonation of the hydrazone by the base, leading to

Scheme 3. (A) DFT Computed Mechanism for the Formation of Thermodynamically Favored 1,2-Dihydronaphthalene (2a) versus the Kinetically Favored 1H-2-Benzoxocin (1a) from Allyl Radical Intermediate D (BP86, def2-TZVP, m4 grid, disp3). Gibbs Free Energies ($\Delta G°_{298\ K}$ in kcal mol^{-1}) Relative to the Energy of Intermediate D. (B) DFT Computed Pathway for Formation of Allyl Radical Intermediate D via a Keto-Enol Mechanism Producing Intermediate C_enol, Followed by HAT via TS8 (BP86, def2-TZVP, m4 grid, disp3). Gibbs Free Energies ($\Delta G°_{298\ K}$ in kcal mol^{-1}) Relative to the Energy of Intermediate C. The Ellipse Represents the Porphyrin Ligand (Tetraphenylporphyrin). Full Atom Models.
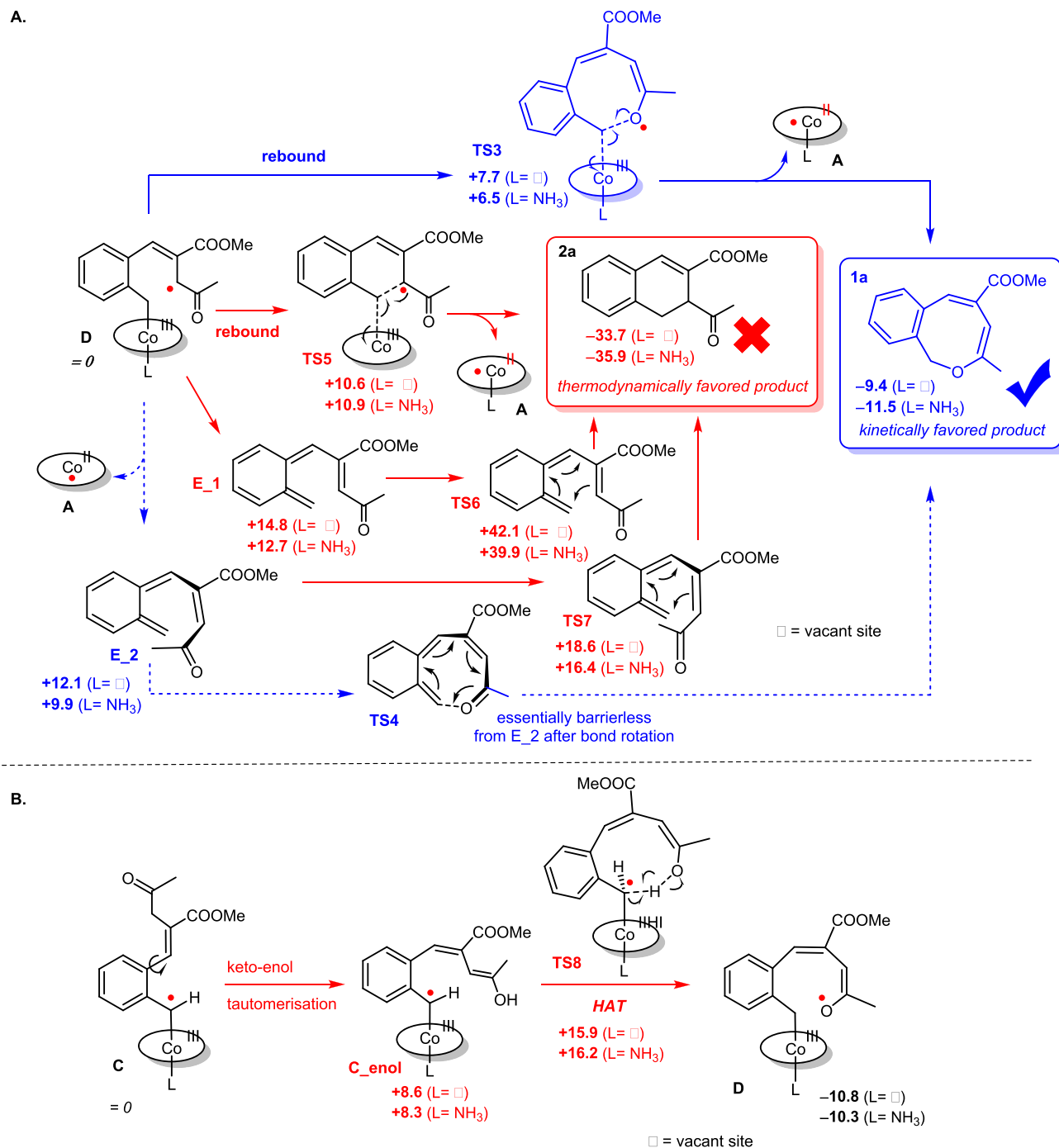
formation of the necessary diazo compound, the cobalt catalyst starts to unveil its unique metallo-radical catalytic trait resulting in formation of the desired medium-sized *O*-heterocyclic products.

We note here that despite [Fe^{II}(ppIX)] (Fe^{II} heme) being known as an active carbene transfer catalyst using diazo compounds,[31] it is ineffective in these reactions (Figure 5A, f). Replacing [Co^{II}(TPP)] by Fe^{II} heme in these reactions (*in situ*

generated by reduction of hemin) leads to the substrate being consumed, but no desired 8-membered ether ring is formed (see Supporting Information for more details), showing that the unique carbene radical species generated at the cobalt(II) catalyst are essential.

In order to confirm the generation of radical species in the pathway, we set a series of radical-trapping experiments with thiol (*t*-butyl thiol), BHT (butylated hydroxytoluene), and BQ

(1,4-benzoquinone), and all these experiments showed obvious reaction inhibition (Figure 5B). Notably, the thiol-trapped intermediate was observed by high-resolution mass spectrometry (HRMS) analysis (see SI for more information).

In an attempt to get more information about the carbene radical intermediate, spin trapping reagent PBN (N-t-butyl-α-phenylnitrone) was used to trap the radical intermediate, and the trapped species was detected with X-band electron paramagnetic resonance (EPR) spectroscopy (Figure 5C). The EPR spectrum displayed an isotropic signal with a triplet of doublets hyperfine pattern ($g = 2.00604$, $A^N = 40.46$ MHz, $A^H = 7.01$ MHz), which is characteristic for a PBN-trapped carbon-centered radical, in agreement with formation of Co(III) radical species in the reaction pathway. Note that the PBN fragment in Figure 5C is drawn attached to the carbene carbon (species **C** trapped by PBN), but it could also be attached to the allylic position (species **D** trapped by PBN), see Supporting Information.

DFT calculations were carried out to gain additional information about the mechanism. Calculations were performed at the BP86/def2-TZVP level of theory, using Grimme's D3 dispersion corrections ("zero" damping), at the doublet spin surface (see Supporting Information for details). This method has been properly benchmarked against experimental data for cobalt(II)-porphyrin systems.[16−20,22−24,32] The proposed mechanism of 1H-2-benzoxocin generation based on our computational studies and experimental observations is shown in Scheme 2.

Since the experimental reaction mixture contains several donor atoms that could potentially bind to cobalt under the catalytic reaction conditions, we explored the DFT mechanism without (green lines in Scheme 2) and with an axial donor bound to cobalt at the sixth coordination site (purple lines). We took NH$_3$ as a model axial ligand, which is a reasonably strong donor ligand and should be representative for axial ligand donor effects of several potential donor ligands (e.g., tosyl hydrazine, MeOH). As is clear from Scheme 2, axial ligand coordination has only a small influence on the reaction profile, and differences in the relative energy barriers with and without NH$_3$ binding are almost negligible (Scheme 2). The same is true for the effect of Ph-substituents at the *meso*-position of the porphyrin ligand (for the DFT calculated energy profile of the reactions using a catalyst without *meso*-Ph-substituents, see Supporting Information). This is confirmed by the experimental results, which also showed that phenyl substituents on the porphyrin of the catalyst are not essential (Table 1, entries 13 and 14, using [Co(ppIX)] and [Co(ppIX-OMe)] as the catalysts).

First, the hydrazone precursor converts to the corresponding diazo compound *in situ*, which is triggered by base in a noncatalyzed pathway. The catalytic cycle starts by trapping of the diazo compound by the cobalt(II) catalyst to produce intermediate **B**. Subsequently, intermediate **B** converts to cobalt(III) carbene radical intermediate **C** by irreversible loss of N$_2$, and simultaneous intramolecular single electron transfer from cobalt(II) to carbon, which is an exergonic pathway with a low energy barrier (without L: +10.9 kcal mol^{-1}; +12.9 kcal mol^{-1} for L = NH$_3$). In the next step, the carbene radical carbon atom abstracts a hydrogen atom from the allylic position of **C** via an intramolecular 1,6-HAT process in **TS2** to produce the delocalized allyl radical intermediate **D**. This is again a process with a low barrier (without L: +9.2 kcal mol^{-1}; +10.7 kcal mol^{-1} for L = NH$_3$). After generation of

intermediate **D**, the carbonyl oxygen atom bearing part of the delocalized radical attacks the carbon bound to cobalt in **TS3**, leading to formation of a new C−O bond with simultaneous homolysis of the Co−C bond to produce the desired final product **1a**. This step is again exergonic, has a low energy barrier (without L: +7.7 kcal mol^{-1}; +6.4 kcal mol^{-1} for L = NH$_3$) and regenerates the cobalt(II) catalyst. The ring-closure step in **TS3** could perhaps also be described as a concerted process involving simultaneous homolysis of the Co−C bond and immediate 8π-cyclization of the thus generated o-QDM intermediate within the coordination sphere of cobalt (see below).

To gain more information about the mechanism, in particular, to find alternative pathways to generate 1H-2-benzoxocins, and to explain why 1H-2-benzoxocins (8-membered rings) are formed instead of the thermodynamically more stable 1,2-dihydronaphthalenes (6-membered rings), we performed additional DFT calculations. In Scheme 3A, we evaluated alternative pathways to form 1H-2-benzoxocins in which the substrate first fully dissociates from the cobalt catalyst, generating a free o-QDM intermediate **E_2** before the ring-closure step (Scheme 3A, dashed blue arrows). Subsequently, the free o-QDM intermediate converts to the final product **1a** via a separate 8π-cyclization step leading rearomatization. Dissociation of o-QDM intermediate **E** from **D** is endergonic (without L: +12.1 kcal mol^{-1}; +9.9 kcal mol^{-1} for L = NH$_3$; i.e., more endergonic than the barrier of **TS3**), while the 8π-cyclization step is essentially barrierless after bond rotation in **E** (the corresponding rotamer of **E** simply collapses to **1a**).[33] The computed mechanisms and energies for 1,2-dihydronaphthalene (**2a**) and 1H-2-benzoxocin (**1a**) formation are also compared. Hypothetical formation of 1,2-dihydronaphthalene **2a** could occur via different pathways. A direct radical rebound over **TS5** from intermediate **D** would produce **2a** in one step (without L: +10.6 kcal mol^{-1}; +10.9 kcal mol^{-1} for L = NH$_3$), but **2a** could also be formed via a 6π-cyclization process in which o-QDM intermediates **E_1** (without L: +14.8 kcal mol^{-1}; +12.7 kcal mol^{-1} for L = NH$_3$) or **E_2** (without L: +12.1 kcal mol^{-1}; +9.9 kcal mol^{-1} for L = NH$_3$) are generated in endergonic processes, respectively, which then convert to **2a** over **TS6** (+27.3 kcal mol^{-1}) or **TS7** (+6.5 kcal mol^{-1}).

As is clear from Scheme 3, all these processes (red pathways) have higher barriers than the pathways leading to 1H-2-benzoxocins **1a** (blue pathways). Formation of the 8-membered enol ether ring products must therefore be kinetically controlled, and the DFT calculations explain the high chemoselectivity for formation of 1H-2-benzoxocins without detectable amounts of the more stable 6-membered dihydronaphthalenes in the experimental reactions (DFT predicted selectivity for 8- versus 6-membered ring formation based on the Eyring equation: $k_{TS3}/k_{TS5} = 134$ without L; $k_{TS3}/k_{TS5} = 1680$ for L = NH$_3$). We believe that the kinetic preference for 8-membered ring formation over 6-membered ring formation in these reactions is at least partially caused by the fact that the aromatic ring and adjacent double bond prevent adaptation of stabilizing boat or chair conformations in the 6-membered transition states **TS5** and **TS6**.

A reaction similar to the computed thermal endergonic ring opening of **1a** to form o-QDM compound **E_2** (+21.4 kcal mol^{-1}) via **TS4**, followed by thermal ring closure of **E_2** to **2a** via **TS7**, readily explains the experimentally observed thermal ring contraction of 8-membered ring compound **19a** to form

the 6-membered dihydronapthalene ring **19ae** upon prolonged heating (Figure 4D, reaction e).

Hypothetically, formation of **1a** could have also proceeded via a keto−enol tautomerization pathway, generating enol compound **C_enol** from **C** followed by radical-type carbene insertion into the O−H bond of **C_enol** (i.e., HAT via **TS8** to form **D**, followed by radical rebound via **TS3**). However, such pathways can be safely excluded based on the high computed reaction barriers of the HAT step (**TS8**) in these pathways (∼16 kcal mol^{-1}, so much larger than **TS2**; see Scheme 3B).

■ CONCLUSIONS

We developed a new catalytic metalloradical protocol for the construction of unprecedented 1*H*-2-benzoxocins. The reaction provides an efficient protocol for the synthesis of medium-sized *O*-heterocyclic rings via cobalt carbene radical intermediates, with a broad substrate scope and an excellent functional group tolerance, and enables the synthesis of a variety of 8-membered cyclic enol ethers in good to excellent yields under mild reaction conditions. The adaptable functionalization of the products showcases the potential for a concise strategy to synthesize a broad range of potentially bioactive structures, containing novel medium-sized hetero-cycles. Thus, formed 1*H*-2-benzoxocins also proved to be useful and versatile platforms to prepare a variety of other potentially bioactive substructures. DFT calculations and spin trapping experiments reveal that cobalt carbene radicals are produced, which are involved in a subsequent intramolecular hydrogen atom transfer step followed by product formation via a radical rebound step. The proposed mechanism and the structure of the reaction products are confirmed by control experiments, 2D-NMR spectroscopy, radical trapping experiments, and X-ray diffraction studies. In contrast to most of the existing strategies for the synthesis of medium-sized ether rings, the newly developed metallo-radical catalyzed protocol enables cyclization of easily accessible linear precursors, is high-yielding, and circumvents the use of scarce precious metal catalysts.

■ ASSOCIATED CONTENT

Ⓢ Supporting Information

The Supporting Information is available free of charge at https://pubs.acs.org/doi/10.1021/jacs.1c10927.

> Experiment details; synthesis procedures; relevant NMR, EPR, HRMS, XRD data; DFT study (PDF)

Accession Codes

CCDC 2093048 contains the supplementary crystallographic data for this paper. These data can be obtained free of charge via www.ccdc.cam.ac.uk/data_request/cif, or by emailing data_request@ccdc.cam.ac.uk, or by contacting The Cambridge Crystallographic Data Centre, 12 Union Road, Cambridge CB2 1EZ, UK; fax: +44 1223 336033.

■ AUTHOR INFORMATION

Corresponding Author

Bas de Bruin − *Homogeneous, Supramolecular and Bio-Inspired Catalysis (HomKat) group, Van 't Hoff Institute for Molecular Sciences (HIMS), University of Amsterdam, 1098 XH Amsterdam, The Netherlands;* ◉ orcid.org/0000-0002-3482-7669; Email: b.debruin@uva.nl

Authors

   Minghui Zhou − *Homogeneous, Supramolecular and Bio-Inspired Catalysis (HomKat) group, Van 't Hoff Institute for Molecular Sciences (HIMS), University of Amsterdam, 1098 XH Amsterdam, The Netherlands*

   Lukas A. Wolzak − *Homogeneous, Supramolecular and Bio-Inspired Catalysis (HomKat) group, Van 't Hoff Institute for Molecular Sciences (HIMS), University of Amsterdam, 1098 XH Amsterdam, The Netherlands*

   Zirui Li − *Department of Bioorganic Synthesis, Leiden Institute of Chemistry, Leiden University, 2333 CC Leiden, The Netherlands;* ◉ orcid.org/0000-0003-0619-6510

   Felix J. de Zwart − *Homogeneous, Supramolecular and Bio-Inspired Catalysis (HomKat) group, Van 't Hoff Institute for Molecular Sciences (HIMS), University of Amsterdam, 1098 XH Amsterdam, The Netherlands;* ◉ orcid.org/0000-0002-0981-1120

   Simon Mathew − *Homogeneous, Supramolecular and Bio-Inspired Catalysis (HomKat) group, Van 't Hoff Institute for Molecular Sciences (HIMS), University of Amsterdam, 1098 XH Amsterdam, The Netherlands;* ◉ orcid.org/0000-0003-2480-3222

Complete contact information is available at:
https://pubs.acs.org/10.1021/jacs.1c10927

Notes

The authors declare no competing financial interest.

■ ACKNOWLEDGMENTS

■ REFERENCES

(1) (a) Rasmussen, S. A.; Andersen, A. J. C.; Andersen, N. G.; Nielsen, K. F.; Hansen, P. J.; Larsen, T. O. Chemical Diversity, Origin, and Analysis of Phycotoxins. *J. Nat. Prod.* **2016**, *79*, 662−673. (b) Truxal, L. T.; Bourdelais, A. J.; Jacocks, H.; Abraham, W. M.; Baden, D. G. Characterization of Tamulamides A and B, Polyethers Isolated from the Marine Dinoflagellate Karenia Brevis. *J. Nat. Prod.* **2010**, *73*, 536−540. (c) Martín, M. J.; Berrué, F.; Amade, P.; Fernández, R.; Francesch, A.; Reyes, F.; Cuevas, C. Halogenated Helianane Derivatives from the Sponge Spirastrella Hartmani. *J. Nat. Prod.* **2005**, *68*, 1554−1555. (d) Martorano, L. H.; Valverde, A. L.; Ribeiro, C. M. R.; De Albuquerque, A. C. F.; Carneiro, J. W. M.; Fiorot, R. G.; Dos Santos Junior, F. M. Unraveling the Helianane Family: A Complementary Quantum Mechanical Study. *New J. Chem.* **2020**, *44*, 8055−8060. (e) Falshaw, C. P.; King, T. J.; Imre, S.; Islimyeli, S.; Thomson, R. H. Laurenyne, a New Acetylene from Laurencia Obtusa: Crystal Structure and Absolute Configuration. *Tetrahedron Lett.* **1980**, *21*, 4951−4954. (f) Irie, T.; Suzuki, M.; Masamune, T. Laurencin, A Constituent from Laurencia Species. *Tetrahedron Lett.* **1965**, *6*, 1091−1099.

(2) (a) Bourdelais, A. J.; Jacocks, H. M.; Wright, J. L. C.; Bigwarfe, P. M.; Baden, D. G. A New Polyether Ladder Compound Produced by the Dinoflagellate Karenia Brevis. *J. Nat. Prod.* **2005**, *68*, 2−6. (b) Friedman, M. A.; Fernandez, M.; Backer, L. C.; Dickey, R. W.; Bernstein, J.; Schrank, K.; Kibler, S.; Stephan, W.; Gribble, M. O.; Bienfang, P.; Bowen, R. E.; Degrasse, S.; Quintana, H. A. F.; Loeffler, C. R.; Weisman, R.; Blythe, D.; Berdalet, E.; Ayyar, R.; Clarkson-

Townsend, D.; Swajian, K.; Benner, R.; Brewer, T.; Fleming, L. E. An Updated Review of Ciguatera Fish Poisoning: Clinical, Epidemiological, Environmental, and Public Health Management. *Mar. Drugs* **2017**, *15*, 72.

(3) (a) Deb, I.; John, S.; Namboothiri, I. N. N. Synthesis of Benzo-Fused Medium Ring Cyclic Ethers via a Michael Addition-Ring Closing Metathesis Strategy Involving Nitroaliphatic Compounds. *Tetrahedron* **2007**, *63*, 11991−11997. (b) Clark, J. S.; Kettle, J. G. Synthesis of Sub-Units of Marine Polycyclic Ethers by Ring-Closing Metathesis and Hydroboration of Enol Ethers. *Tetrahedron* **1999**, *55*, 8231−8248. (c) Brown, R. C. D.; Satcharoen, V. Ring-Closing Metathesis of Hetereoation-Substituted Dienes. *Heterocycles* **2006**, *70*, 705−736. (d) Prunet, J. Progress in Metathesis through Natural Product Synthesis. *Eur. J. Org. Chem.* **2011**, *2011*, 3634−3647. (e) Green, J. C.; Jiménez-Alonso, S.; Brown, E. R.; Pettus, T. R. R. Total Synthesis and Repudiation of the Helianane Family. *Org. Lett.* **2011**, *13*, 5500−5503. (f) Ortega, N.; Martín, T.; Martín, V. S. Stereoselective Synthesis of Eight-Membered Cyclic Ethers by Tandem Nicholas Reaction/Ring-Closing Metathesis: A Short Synthesis of (+)-Cis-Lauthisan. *Org. Lett.* **2006**, *8*, 871−873.

(4) (a) Clark, J. S.; Holmes, A. B. A Strategy for the Asymmetric Synthesis of Medium Ring Oxygen Heterocycles: Enantioselective Total Synthesis of (+)-Octahydrodeacetyldebromolaurencin. *Tetrahedron Lett.* **1988**, *29*, 4333−4336. (b) McGarry, D. G.; Somers, P. K.; Kim, B. H.; Ogilvie, W. W.; Yiannikouros, G.; Prasad, C. V. C.; Veale, C. A.; Hark, R. R.; Nicolaou, K. C. Synthesis of Medium-Sized Ring Ethers from Thionolactones. Applications to Polyether Synthesis. *J. Am. Chem. Soc.* **1990**, *112*, 6263−6276. (c) Burton, J. W.; Clark, J. S.; Derrer, S.; Stork, T. C.; Bendall, J. G.; Holmes, A. B. Synthesis of Medium Ring Ethers. 5. The Synthesis of (±)-Laurencin. *J. Am. Chem. Soc.* **1997**, *119*, 7483−7498.

(5) (a) Nicolaou, K. C.; Hwang, C. K.; Duggan, M. E.; Nugiel, D. A.; Abe, Y.; Reddy, K. B.; DeFrees, S. A.; Reddy, D. R.; Awartani, R. A.; Conley, S. R.; Rutjes, F. P. J. T.; Theodorakis, E. A. Total Synthesis of Brevetoxin B. 1. First Generation Strategies and New Approaches to Oxepane Systems. *J. Am. Chem. Soc.* **1995**, *117*, 10227−10238. (b) Nicolaou, K. C.; Hwang, C. K.; Nugiel, D. A. Synthetic Studies on the Dioxepane Region of Brevetoxin B. New Synthetic Technology for the Construction of Oxepanes and Synthesis of a Model for the CDEF Ring Skeleton of Brevetoxin B. *J. Am. Chem. Soc.* **1989**, *111*, 4136−4137. (c) Carreno, M. C.; Des Mazery, R.; Urbano, A.; Colobert, F.; Solladie, G. Enantioselective Access to 2,7-Cis-Disubstituted Oxepanes: Formal Synthesis of (+)-Isolaurepan. *Org. Lett.* **2004**, *6*, 297−299. (d) Carreno, M. C.; Des Mazery, R.; Urbano, A.; Colobert, F.; Solladie, G. Short Asymmetric Synthesis of (−)- and (+)-cis-Lauthisan. *Org. Lett.* **2005**, *7*, 2039−2042.

(6) Tamiya, H.; Goto, K.; Matsuda, F. Efficient Medium-Ring Cyclization under Non-High-Dilution Conditions Using SmI$_2$. *Org. Lett.* **2004**, *6*, 545−547.

(7) Sabui, S. K.; Venkateswaran, R. V. Synthesis of Helianane, an Unusual Marine Sesquiterpene Employing Ring-Expansion by Flash Vacuum Thermolysis. *Tetrahedron Lett.* **2004**, *45*, 9653−9655.

(8) Hamura, T.; Kawano, N.; Matsumoto, T.; Suzuki, K. Peri-Selectivity in Thermolysis of Acyloxybenzocyclobutenes Possessing α,β-Unsaturated Carbonyl Group: Synthesis of 2-Benzoxocin Derivatives. *Chem. Lett.* **2006**, *35*, 730−731.

(9) Chattopadhyay, P.; Mukherjee, M.; Ghosh, S. A Simple Construction of Chiral Fused Benzoxocine Ring Ethers from D-Glucose by Regioselective 8-Endo-Aryl Radical Cyclisation. *Chem. Commun.* **1997**, *90*, 2139−2140.

(10) Boeckman, R. K.; Shair, M. D.; Vargas, J. R.; Stolz, L. A. Synthetic and Mechanistic Studies of the Retro-Claisen Rearrangement. 2. A Facile Route to Medium-Ring Heterocycles via Rearrangement of Vinylcyclopropane and Cyclobutanecarboxaldehydes. *J. Org. Chem.* **1993**, *58*, 1295−1297.

(11) (a) Narayanam, J. M.; Stephenson, C. R. Visible Light Photoredox Catalysis: Applications in Organic Synthesis. *Chem. Soc. Rev.* **2011**, *40*, 102−113. (b) Quiclet-Sire, B.; Zard, S. Z. Fun with Radicals: Some New Perspectives for Organic Synthesis. *Pure Appl.*

Chem. **2010**, *83*, 519−551. (c) Prier, C. K.; Rankic, D. A.; MacMillan, D. W. Visible Light Photoredox Catalysis with Transition Metal Complexes: Applications in Organic Synthesis. *Chem. Rev.* **2013**, *113*, 5322−5363. (d) Studer, A.; Curran, D. P. Catalysis of Radical Reactions: A Radical Chemistry Perspective. *Angew. Chem., Int. Ed.* **2016**, *55*, 58−102. (e) Gansäuer, A.; Behlendorf, M.; Von Laufenberg, D.; Fleckhaus, A.; Kube, C.; Sadasivam, D. V.; Flowers, R. A. Catalytic, Atom-Economical Radical Arylation of Epoxides. *Angew. Chem., Int. Ed.* **2012**, *51*, 4739−4742. (f) Gansäuer, A.; Hildebrandt, S.; Michelmann, A.; Dahmen, T.; von Laufenberg, D.; Kube, C.; Fianu, G. D.; Flowers, R. A. Cationic Titanocene(III) Complexes for Catalysis in Single-Electron Steps. *Angew. Chem., Int. Ed.* **2015**, *54*, 7003−7006. (g) Mühlhaus, F.; Weißbarth, H.; Dahmen, T.; Schnakenburg, G.; Gansäuer, A. Merging Regiodivergent Catalysis with Atom-Economical Radical Arylation. *Angew. Chem., Int. Ed.* **2019**, *58*, 14208. (h) Gansäuer, A.; Shi, L.; Otte, M. Catalytic Enantioselective Radical Cyclization via Regiodivergent Epoxide Opening. *J. Am. Chem. Soc.* **2010**, *132*, 11858. (i) Gansäuer, A.; Otte, M.; Shi, L. Radical Cyclizations Terminated by Ir-Catalyzed Hydrogen Atom Transfer. *J. Am. Chem. Soc.* **2011**, *133*, 416−417. (j) Yao, C.; Dahmen, T.; Gansäuer, A.; Norton, J. Anti-Markovnikov alcohols via epoxide hydrogenation through cooperative catalysis. *Science* **2019**, *364*, 764−767.

(12) (a) Luca, O. R.; Crabtree, R. H. Redox-Active Ligands in Catalysis. *Chem. Soc. Rev.* **2013**, *42*, 1440−1459. (b) Dzik, W. I.; Zhang, X. P.; de Bruin, B. Redox Noninnocence of Carbene Ligands: Carbene Radicals in (Catalytic) C-C Bond Formation. *Inorg. Chem.* **2011**, *50*, 9896−9903. (c) Goswami, M.; Lyaskovskyy, V.; Domingos, S. R.; Buma, W. J.; Woutersen, S.; Troeppner, O.; Ivanović-Burmazović, I.; Lu, H.; Cui, X.; Zhang, X. P.; Reijerse, E. J.; DeBeer, S.; van Schooneveld, M. M.; Pfaff, F. F.; Ray, K.; de Bruin, B. Characterization of Porphyrin-Co(III)-'nitrene Radical' Species Relevant in Catalytic Nitrene Transfer Reactions. *J. Am. Chem. Soc.* **2015**, *137*, 5468−5479.

(13) (a) Roy, S.; Das, S. K.; Chattopadhyay, B. Cobalt(II)-Based Metalloradical Activation of 2-(Diazomethyl)Pyridines for Radical Transannulation and Cyclopropanation. *Angew. Chem., Int. Ed.* **2018**, *57*, 2238−2243. (b) Xia, Y.; Wang, J. N-Tosylhydrazones: Versatile Synthons in the Construction of Cyclic Compounds. *Chem. Soc. Rev.* **2017**, *46*, 2306−2362. (c) Bamford, W. R.; Stevens, T. S. *J. Chem. Soc.* **1952**, 4735−4740. (d) Reddy, A. R.; Zhou, C. Y.; Guo, Z.; Wei, J.; Che, C. M. Ruthenium-Porphyrin-Catalyzed Diastereoselective Intramolecular Alkyl Carbene Insertion into C-H Bonds of Alkyl Diazomethanes Generated in Situ from N-Tosylhydrazones. *Angew. Chem., Int. Ed.* **2014**, *53*, 14175−14180.

(14) (a) Goswami, M.; de Bruin, B.; Dzik, W. I. Difluorocarbene Transfer from a Cobalt Complex to an Electron-Deficient Alkene. *Chem. Commun.* **2017**, *53*, 4382−4385. (b) Chirila, A.; Gopal Das, B.; Paul, N. D.; de Bruin, B. Diastereoselective Radical-Type Cyclopropanation of Electron-Deficient Alkenes Mediated by the Highly Active Cobalt(II) Tetramethyltetraaza[14]Annulene Catalyst. *ChemCatChem* **2017**, *9*, 1413−1421. (c) Intrieri, D.; Caselli, A.; Gallo, E. Cyclopropanation Reactions Mediated by Group 9 Metal Porphyrin Complexes. *Eur. J. Inorg. Chem.* **2011**, *2011*, 5071−5081. (d) Zhu, S.; Ruppel, J. V.; Lu, H.; Wojtas, L.; Zhang, X. P. Cobalt-Catalyzed Asymmetric Cyclopropanation with Diazosulfones: Rigidification and Polarization of Ligand Chiral Environment via Hydrogen Bonding and Cyclization. *J. Am. Chem. Soc.* **2008**, *130*, 5042−5043. (e) Huang, L.; Chen, Y.; Gao, G. Y.; Zhang, X. P. Diastereoselective and Enantioselective Cyclopropanation of Alkenes Catalyzed by Cobalt Porphyrins. *J. Org. Chem.* **2003**, *68*, 8179−8184. (f) Lee, W. C. C.; Wang, D. S.; Zhang, C.; Xie, J.; Li, B.; Zhang, X. P. Asymmetric Radical Cyclopropanation of Dehydroaminocarboxylates: Stereoselective Synthesis of Cyclopropyl α-Amino Acids. *Chem.* **2021**, *7*, 1588.

(15) Cui, X.; Xu, X.; Wojtas, L.; Kim, M. M.; Zhang, X. P. Regioselective Synthesis of Multisubstituted Furans via Metalloradical Cyclization of Alkynes with α-Diazocarbonyls: Construction of

Functionalized α-Oligofurans. *J. Am. Chem. Soc.* **2012**, *134*, 19981−19984.

(16) Das, B. G.; Chirila, A.; Tromp, M.; Reek, J. N. H.; de Bruin, B. Co^{III}−Carbene Radical Approach to Substituted *1H*-Indenes. *J. Am. Chem. Soc.* **2016**, *138*, 8968−8975.

(17) (a) Wen, X.; Wang, Y.; Zhang, X. P. Enantioselective Radical Process for Synthesis of Chiral Indolines by Metalloradical Alkylation of Diverse C(sp^3)-H Bonds. *Chem. Sci.* **2018**, *9*, 5082−5086. (b) Karns, A. S.; Goswami, M.; de Bruin, B. Catalytic Synthesis of Indolines by Hydrogen Atom Transfer to Cobalt(III)−Carbene Radicals. *Chem. - Eur. J.* **2018**, *24*, 5253−5258.

(18) (a) Paul, N. D.; Chirila, A.; Lu, H.; Zhang, X. P.; de Bruin, B. Carbene Radicals in Cobalt(II)-Porphyrin-Catalysed Carbene Carbonylation Reactions; A Catalytic Approach to Ketenes. *Chem. - Eur. J.* **2013**, *19*, 12953−12958. (b) Chirila, A.; van Vliet, K. M.; Paul, N. D.; de Bruin, B. [Co(MeTAA)] Metalloradical Catalytic Route to Ketenes via Carbonylation of Carbene Radicals. *Eur. J. Inorg. Chem.* **2018**, *2018*, 2251−2258.

(19) te Grotenhuis, C.; Das, B. G.; Kuijpers, P. F.; Hageman, W.; Trouwborst, M.; de Bruin, B. Catalytic 1,2-Dihydronaphthalene and: *E*-Aryl-Diene Synthesis via Co^{III}-Carbene Radical and *o*-Quinodimethane Intermediates. *Chem. Sci.* **2017**, *8*, 8221−8230.

(20) Lankelma, M.; Olivares, A. M.; de Bruin, B. [Co(TPP)]-Catalyzed Formation of Substituted Piperidines. *Chem. - Eur. J.* **2019**, *25*, 5658−5663.

(21) Wang, Y.; Wen, X.; Cui, X.; Zhang, X. P. Enantioselective Radical Cyclization for Construction of 5-Membered Ring Structures by Metalloradical Alkylation. *J. Am. Chem. Soc.* **2018**, *140*, 4792−4796.

(22) (a) Majumdar, N.; Paul, N. D.; Mandal, S.; de Bruin, B.; Wulff, W. D. Catalytic Synthesis of *2H*-Chromenes. *ACS Catal.* **2015**, *5* (4), 2329−2366. (b) Paul, N. D.; Mandal, S.; Otte, M.; Cui, X.; Zhang, X. P.; de Bruin, B. Metalloradical Approach to *2H*-Chromenes. *J. Am. Chem. Soc.* **2014**, *136*, 1090−1096.

(23) te Grotenhuis, C.; van den Heuvel, N.; van der Vlugt, J. I.; de Bruin, B. Catalytic Dibenzocyclooctene Synthesis via Cobalt(III)−Carbene Radical and *ortho*-Quinodimethane Intermediates. *Angew. Chem., Int. Ed.* **2018**, *57*, 140−145.

(24) Zhou, M.; Lankelma, M.; van der Vlugt, J. I.; de Bruin, B. Catalytic Synthesis of 8-Membered Ring Compounds via Cobalt(III)-Carbene Radicals. *Angew. Chem., Int. Ed.* **2020**, *59*, 11073−11079.

(25) Cho, C. S.; Lim, D. K.; Zhang, J. Q.; Kim, T. J.; Shim, S. C. Palladium-Catalyzed Tandem Heck and Aldol Reactions between 2-Bromobenzaldehydes and Functionalized Alkenes Leading to Naphthalenes. *Tetrahedron Lett.* **2004**, *45*, 5653−5656.

(26) (a) Padwa, A. Generation and utilization of carbonyl ylides via the tandem cyclization-cycloaddition. *Acc. Chem. Res.* **1991**, *24* (1), 22−28. (b) Vinas-Lobez, J.; Levitre, G.; de Aguirre, A.; Besnard, C.; Poblador-Bahamonde, A. I.; Lacour, J. Enabling Cyclization Strategies through Carbonyl-Ylide-Mediated Synthesis. *ACS Org. Inorg. Au* **2021**, *1*, 11−17.

(27) Lower yields of the *1H*-2-benzoxocins for these reactions are due to the generation of a slightly higher amount of the aromatic aldol side-product.

(28) (a) Lee, S. Y.; Moon, E.; Kim, S. Y.; Choi, S. U.; Lee, K. R. Quinone Derivatives from the Rhizomes of Acorus Gramineus and Their Biological Activities. *Biosci., Biotechnol., Biochem.* **2013**, *77*, 276−280. (b) Nono, E. C. N.; Mkounga, P.; Kuete, V.; Marat, K.; Hultin, P. G.; Nkengfack, A. E. Pycnanthulignenes A-D, Antimicrobial Cyclolignene Derivatives from the Roots of Pycnanthus Angolensis. *J. Nat. Prod.* **2010**, *73*, 213−216. (c) Hejtmánková, L.; Jirman, J.; Sedlák, M. Synthesis and Dehydration Reaction of 1-(4)-Benzyloxyphenyl)-6-Methoxy-2-Phenyl-1,2,3,4-Tetrahydronaphth-2-Ol: Possible Intermediate of Lasofoxifene. *Res. Chem. Intermed.* **2009**, *35*, 615−623. (d) Viana, G. S. B.; Bandeira, M. A. M.; Matos, F. J. A. Analgesic and Antiinflammatory Effects of Chalcones Isolated from Myracrodruon Urundeuva Allemão. *Phytomedicine* **2003**, *10*, 189−195.

(29) (a) Lei, H.; Lin, X.; Han, L.; Ma, J.; Dong, K.; Wang, X.; Zhong, J.; Mu, Y.; Liu, Y.; Huang, X. Polyketide Derivatives from a Marine-Sponge-Associated Fungus Pestalotiopsis Heterocornis. *Phytochemistry* **2017**, *142*, 51−59. (b) Wang, J.; Wei, X.; Qin, X.; Chen, H.; Lin, X.; Zhang, T.; Yang, X.; Liao, S.; Yang, B.; Liu, J.; Zhou, X.; Tu, Z.; Liu, Y. Two New Prenylated Phenols from Endogenous Fungus Pestalotiopsis Vaccinii of Mangrove Plant Kandelia Candel (L.) Druce. *Phytochem. Lett.* **2015**, *12*, 59−62.

(30) (a) Guo, Y.; Ding, L.; Ghidinelli, S.; Gotfredsen, C. H.; de la Cruz, M.; Mackenzie, T. A.; Ramos, M. C.; Sánchez, P.; Vicente, F.; Genilloud, O.; Coriani, S.; Larsen, R. W.; Frisvad, J. C.; Larsen, T. O. Taxonomy Driven Discovery of Polyketides From Aspergillus Californicus. *J. Nat. Prod.* **2021**, *84*, 979−985. (b) Saito, T.; Itabashi, T.; Wakana, D.; Takeda, H.; Yaguchi, T.; Kawai, K. I.; Hosoe, T. Isolation and Structure Elucidation of New Phthalide and Phthalane Derivatives, Isolated as Antimicrobial Agents from Emericella Sp. IFM57991. *J. Antibiot.* **2016**, *69*, 89−96. (c) Lei, H.; Lei, J.; Zhou, X.; Hu, M.; Niu, H.; Song, C.; Chen, S.; Liu, Y.; Zhang, D. Cytotoxic Polyketides from the Marine Sponge-Derived Fungus Pestalotiopsis Heterocornis XWS03F09. *Molecules* **2019**, *24*, 2655. (d) Kesting, J. R.; Olsen, L.; Staerk, D.; Tejesvi, M. V.; Kini, K. R.; Prakash, H. S.; Jaroszewski, J. W. Production of Unusual Dispiro Metabolites in Pestalotiopsis Virgatula Endophyte Cultures: HPLC-SPE-NMR, Electronic Circular Dichroism, and Time-Dependent Density-Functional Computation Study. *J. Nat. Prod.* **2011**, *74*, 2206−2215.

(31) (a) Tinoco, A.; Wei, Y.; Bacik, J. P.; Carminati, D. M.; Moore, E. J.; Ando, N.; Zhang, Y.; Fasan, R. Origin of High Stereocontrol in Olefin Cyclopropanation Catalyzed by an Engineered Carbene Transferase. *ACS Catal.* **2019**, *9*, 1514−1524. (b) Bordeaux, M.; Tyagi, V.; Fasan, R. Highly Diastereoselective and Enantioselective Olefin Cyclopropanation Using Engineered Myoglobin-Based Catalysts. *Angew. Chem., Int. Ed.* **2015**, *54*, 1744−1748. (c) Villarino, L.; Splan, K. E.; Reddem, E.; Alonso-Cotchico, L.; Gutiérrez de Souza, C.; Lledós, A.; Maréchal, J. D.; Thunnissen, A. M. W. H.; Roelfes, G. An Artificial Heme Enzyme for Cyclopropanation Reactions. *Angew. Chem., Int. Ed.* **2018**, *57*, 7785−7789. (d) Wang, Z. J.; Peck, N. E.; Renata, H.; Arnold, F. H. Cytochrome P450-Catalyzed Insertion of Carbenoids into N-H Bonds. *Chem. Sci.* **2014**, *5*, 598−601. (e) Weissenborn, M. J.; Löw, S. A.; Borlinghaus, N.; Kuhn, M.; Kummer, S.; Rami, F.; Plietker, B.; Hauer, B. Enzyme-Catalyzed Carbonyl Olefination by the E. Coli Protein YfeX in the Absence of Phosphines. *ChemCatChem* **2016**, *8*, 1636−1640.

(32) (a) de Bruin, B.; Dzik, W. I.; Li, S.; Wayland, B. B. Hydrogen-Atom Transfer in Reactions of Organic Radicals with [Co^{II}(por)]. (por = Porphyrinato) and in Subsequent Addition of [Co(H)(por)] to Olefins. *Chem. - Eur. J.* **2009**, *15*, 4312−4320. (b) Li, S.; Peng, C. H.; Fryd, M.; Wayland, B. B.; de Bruin, B. Exchange of Organic Radicals with Organo-Cobalt Complexes Formed in the Living Radical Polymerization of Vinyl Acetate. *J. Am. Chem. Soc.* **2008**, *130*, 13373−13381. (c) Kuijpers, P. F.; Tiekink, M. J.; Breukelaar, W. B.; Broere, D. L. J.; van Leest, N. P.; van der Vlugt, J. I.; Reek, J. N. H.; de Bruin, B. Nitrene-radical approach to Saturated Heterocycles; Cobalt Porphyrin Catalysed Intramolecular Ring-Closing C-H Amination of Aliphatic Azides. *Chem. - Eur. J.* **2017**, *23*, 7945−7952. (d) Dzik, W. I.; Xu, X.; Zhang, X. P.; Reek, J. N. H.; de Bruin, B. Carbene Radicals in Co^{II}(Por)-Catalyzed Olefin Cyclopropanation. *J. Am. Chem. Soc.* **2010**, *132*, 10891−10902. (e) Lyaskovskyy, V.; Suarez, A. I. O.; Lu, H.; Jiang, H.; Zhang, X. P.; de Bruin, B. Mechanism of Cobalt(II) Porphyrin-Catalyzed C-H Amination with Organic Azides: Radical Nature and H-Atom Abstraction Ability of the Key Cobalt(III)-Nitrene Intermediates. *J. Am. Chem. Soc.* **2011**, *133*, 12264−12273.

(33) DFT calculations at the b3-lyp level did allow us to find a low-barrier transition state **TS4** between rotamer **E_3** and **1a**, but this functional strongly underestimates the Co−C bond strengths and is therefore unsuitable for full pathway calculations of these cobalt systems (see SI for more information).